Ionizing radiation induces long-term senescence in endothelial cells through mitochondrial respiratory complex II dysfunction and superoxide generation

Audrey Lafargue, Charlotte Degorre, Isabelle Corre, Marie-Clotilde Alves-Guerra, Marie-Hélène Gaugler, François Vallette, Claire Pecqueur, François Paris

Ionizing radiation induces long-term senescence in endothelial cells through mitochondrial respiratory complex II dysfunction and superoxide generation

Audrey Lafargue, Charlotte Degorre, Isabelle Corre, Marie-Clotilde Alves-Guerra, Marie-Hélène Gaugler, François Vallette, Claire Pecqueur, François Paris

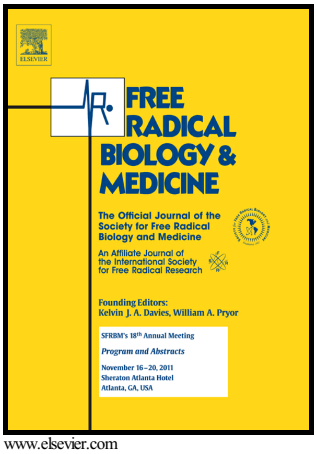

www.elsevier.com

PII: S0891-5849(17)30222-8
DOI: http://dx.doi.org/10.1016/j.freeradbiomed.2017.04.019
Reference: FRB13300

To appear in: *Free Radical Biology and Medicine*

Received date: 21 November 2016
Revised date: 1 April 2017
Accepted date: 16 April 2017

Cite this article as: Audrey Lafargue, Charlotte Degorre, Isabelle Corre, Marie Clotilde Alves-Guerra, Marie-Hélène Gaugler, François Vallette, Claire Pecqueur and François Paris, Ionizing radiation induces long-term senescence i endothelial cells through mitochondrial respiratory complex II dysfunction an superoxide generation, *Free Radical Biology and Medicine* http://dx.doi.org/10.1016/j.freeradbiomed.2017.04.019

Ionizing radiation induces long-term senescence in endothelial cells through mitochondrial respiratory complex II dysfunction and superoxide generation

Audrey Lafargue[a,b,c,#], Charlotte Degorre[a,b,c,#], Isabelle Corre[a,b,c], Marie-Clotilde Alves-Guerra[d,e,f], Marie-Hélène Gaugler[a,b,c], François Vallette[a,b,c,g], Claire Pecqueur[a,b,c], and François Paris[a,b,c,g,*]

Affiliations

[a]Inserm, UMR1232, Nantes, F-44000, France.

[b]Université de Nantes, Nantes, F-44000, France.

[c]CNRS, UMR 6299, Nantes, F-44000, France.

[d]Inserm UMR1016, Paris, F-75014, France.

[e]CNRS UMR8104, Paris, F-75014, France.

[f]Université Paris Descartes, Paris, F-75014, France.

[g]Institut de Cancérologie de l'Ouest, Saint-Herblain, F-44800, France.

[*]Corresponding author

[#]Co-authorship

Address

François Paris, Ph.D.

Centre de Recherche en Cancérologie Nantes-Angers, UMR Inserm 892 CNRS 6299, IRS-UN, 8 quai Moncousu, BP 70721, 44007 Nantes Cedex 01, France.

Phone: +33 228080302 ; Fax: +33 228080302 ; email: francois.paris@inserm.fr

Running title

Deciphering radiation-induced endothelial senescence

Number of words: 5339

Number of figures: 7

Abbreviations

Senescence, endothelial cell, mitochondrial oxidative stress, ionizing radiation

Abstract

Ionizing radiation causes oxidative stress, leading to acute and late cellular responses. We previously demonstrated that irradiation of non-proliferating endothelial cells, as observed in normal tissues, induces early apoptosis, which can be inhibited by pretreatment with Sphingosine-1-Phosphate. We now propose to better characterize the long-term radiation response of endothelial cells by studying the molecular pathways associated with senescence and its link with acute apoptosis. First, senescence was validated in irradiated quiescent microvascular HMVEC-L in a dose- and time-dependent manner by SA β-galactosidase staining, $p16^{Ink4a}$ and $p21^{Waf1}$ expression, pro-inflammatory IL-8 secretion and DNA damage response activation. This premature aging was induced independently of Sphingosine 1-Phosphate treatment, supporting its non-connection with acute IR-induced apoptosis. Then, senescence under these conditions showed persistent activation of p53 pathway and mitochondrial dysfunctions, characterized by O2•- generation, inhibition of respiratory complex II activity and over-expression of SOD2 and GPX1 detoxification enzymes. Senescence was significantly inhibited by treatment with pifithrin–α, a p53 inhibitor, or by MnTBAP, a superoxide dismutase mimetic, validating those molecular actors in IR-induced endothelial cell aging. However, MnTBAP, but not pifithrin–α, was able to limit superoxide generation and to rescue the respiratory complex II activity. Furthermore, MnTBAP was not modulating p53 up-regulation, suggesting that IR-induced senescence in quiescent endothelial cells is provided by at least 2 different pathways dependent of the mitochondrial oxidative stress response and the p53 activation. Further characterization of the actors involved in the respiratory complex II dysfunction will open new pharmacological strategies to modulate late radiation toxicity.

Highlights

- Ionizing radiation induces long-term senescence in non-proliferating endothelial cells
- Apoptosis inhibition by Sphingosine 1-phosphate does not modulate senescence
- p53 activity, mitochondrial superoxide generation and loss of respiratory complex II activity are observed during senescence
- Superoxide dismutase mimetic or pharmacological inhibition of p53 activation prevents senescence
- SOD mimetic, but not p53 inhibition, blocks superoxide generation and revert respiratory complex II dysfunction

Keywords

Senescence, endothelial cell, mitochondrial oxidative stress, ionizing radiation

1. Introduction

Radiotherapy is a foremost weapon to fight cancer progression through the promotion of deadly oxidative stress in the tumor cells. However, it is also known to potentially induce major acute and chronic side-effects in irradiated normal tissues in the periphery of the tumor, leading to pathogenesis including tissue necrosis, fibrosis, atrophy, atherosclerosis, or heart failure [1]. Deciphering the multicellular and molecular mechanisms in normal tissue radiation response will permit new pharmacological strategies to limit those radiation toxicities.

Within the complexity of molecular and cellular mechanisms, endothelium network is regarded as a major player in radiation toxicities [2, 3]. The response of the vasculature to radiation can be defined as early and late effects, according to the appearance of the tissular damage. Microvascular endothelial cell apoptosis after high dose of radiation constitutes a primary lesion involved in acute organ failure, including gastrointestinal syndrome [4], blood-spinal cord brain barrier breakdown [5], central nervous syndrome [6], and parotid gland hypo-salivation [7]. Cell death is triggered by the sphingolipid ceramide generated upon hydrolysis of sphingomyelin by acid sphingomyelinase [4]. Pharmacological treatment with Sphingosine 1-phosphate (S1P), a ceramide metabolite with antagonist properties, blocks irradiation (IR)-induced microvascular endothelial cell apoptosis, inhibiting small intestine necrosis [4, 8]. On the other hand, IR induces late persistent endothelial dysfunctions, including microvessel collapse and activated phenotype, and ultimately premature aging and senescence [2]. These effects impact normal tissue homeostasis leading to ischemia or fibrosis through increase of hypoxia and inflammation [1].

Senescence, a notable long-term cell dysfunction induced by ionizing radiation, contributes to age-related diseases [9]. Senescent cells are characterized by their inability to cycle and the up-

regulation of senescence-associated β-galactosidase (SA β-gal) staining. Two types of senescence have been described: the replicative senescence, occurring after high number of cell division leading to mitosis exhaustion and the premature senescence appearing in response to genotoxic or oncogenic stress [9]. Several molecular pathways are ubiquitously triggered during aging process. DNA damage and its signaling response generated by a high level of intracellular reactive oxygen species (ROS) remain activated during senescence. DNA damage response (DDR) is initiated by the phosphorylation of the phosphatidylinositol 3-kinase-related protein kinases (ATM, ATR and DNA-PKcs), activating a stress response signaling involving γH2AX histone, cell cycle modulator Chk1 and Chk2 proteins and p53 [10]. Then, senescence-induced cell cycle arrest is under the control of p53 and/or $p16^{Ink4a}$ activities leading respectively to $p21^{Waf1}$ over-expression and to retinoblastoma hypo-phosphorylation. Finally, the maintenance of a senescence-associated secretory phenotype (SASP) also represents a hallmark of senescence. This secretome includes pro-inflammatory cytokines, such as interleukin (IL)-1, 6, 8 and TNF-α, and occurs after the establishment of the persistent DDR signaling [11].

After exposure to various stresses, endothelial cells may undergo senescence that leads to vascular dysfunctions. Premature aging in macrovascular HUVEC impairs angiogenesis after alteration of mitochondrial redox state, through the repression of pro-survival Bcl-2 removing antioxidant glutathione from the mitochondrial membrane and leading to ROS generation [12]. Ionizing radiation or oxidative stress induces a premature senescence in macrovascular HUVEC, BAEC and cerebromicrovascular CMVEC models with a long-term persistence of DDR and SASP [13-15]. Proteomic analysis of senescent HUVEC after low dose irradiation showed an up-regulation of the p53/$p21^{Waf1}$ pathway [16]. Furthermore, invalidation of p53 by siRNA also inhibited senescence in microvascular HMVEC-L after exposure to 4 Gy [17]. However,

proliferating status of those endothelial cell models have limited significance to physiopathology since cell division in normal vessels occurs rarely, every 1 to 3 years [18]. Senescence, in those studies, was observed within the first weeks after IR while vascular dysfunctions appeared after weeks or even months later. Furthermore, molecular mechanisms inducing IR-induced senescence in quiescent microvascular endothelial cells, predominant in normal tissues, remains totally unknown and may involve actors different from those previously described in proliferative macrovascular endothelial cells [12].

The present manuscript aims at better characterizing IR-induced long-term senescence in non-proliferating endothelial cells. The link between acute death and long-term premature aging will be defined after blocking apoptosis by S1P pretreatment. Then, senescence will be deciphered through the characterization of some foremost actors of the molecular cascade, comprising p53 overexpression, dysfunction of the respiratory chain complex II (Cplx II) of the mitochondria and the generation of O_2•-. Finally, pharmacological inhibition of those actors will permit to validate and order the signaling pathways involved in the IR-induced quiescent endothelial cell senescence.

2. Materials & Methods

2.1. Cell culture and treatments

Primary Human Lung Microvascular Endothelial Cell, HMVEC-L (primary human cells, female, Caucasian, 34 years old) were seeded at 5000 cells/cm² in EBM-2 with 5% FBS and EGM-2 supplement (all products, Lonza Bioscience) until reaching complete confluence. Medium was changed for low serum EBM-2 with 0.1% FBS 18h before IR. One µM S1P (Aventi polar Lipids) or its vehicle (PET; prepared as described [19]) was added 2h before IR ranging to 15 Gy with a CP-160 irradiator (Faxitron X-ray Corp.). Low-serum medium was replaced by complete EBM-2 2h after IR, and then weekly. Cell cultures were maintained for 28 days. Non-toxic concentration of pifithrin-α (PFT-α; 10µM; Sigma-Aldrich), KU55933 (5µM; Selleckchem), N-acetyl-cystein (NAC; 1mM; Sigma-Aldrich), or Manganese (III) tetrakis (4-benzoic acid) porphyrin chloride (MnTBAP; 1µM; Merck) were added at day 4, 7, 10, 13, 16, 19, and 21 post-IR.

2.2. Cellular death assay

As described [20], death fraction was estimated on Malassez slides by the ratio of floating cell number to total cell number (floating + adherent). Floating cell population represented the non-adherent cells in the culture medium and the loosely adherent cells issued from PBS washes of the monolayer.

2.3. Senescence-associated β-Galactosidase assay

As described [21], 4% paraformaldehyde (PFA)-fixed cells in 6-well plates were incubated O/N without CO_2 at 37°C with SA β-galactosidase staining solution (1mg/ml 5-bromo-4-chloro-3-

indolyl-β-D-galactopyranoside or X-gal; 5mM potassium ferrocyanide; 2mM MgCl2; 150mM NaCl; 40mM citric acid; 12mM NaH2PO4; Sigma-Aldrich. Images were captured under optical microscopy (DM IRB; Leica; x200 magnification). SA β-gal-positive cells (blue staining) were reported on the total cell number per field representing a mean of 150 cells (3 independent wells per experiment).

2.4. Western blot analysis and quantification

Twenty µg of HMVEC-L proteins were separated by SDS-PAGE and transferred to PVDF Immobilon-P membranes (Millipore). Milk 5% or WBR (Roche) saturated membranes were hybridized O/N at 4°C with a primary antibody, and with a HRP-coupled secondary antibody. Proteins of interest were revealed by Clarity Western Blot ECL substrate (Biorad). Primary antibodies were directed against $p21^{Waf1}$ and $p16^{Ink4a}$ (respectively 556430, 554079; BD); p53 and Bcl-2 (M7001, mo897; Dako); actin (05-636, MAB1501; Millipore); MDM2 (AF1244; R&D); ATM (GTX70103, GenTex); phospho-Ser1981 ATM (DR1002; Calbiochem); total and phospho-Ser2056 DNA-PKcs, SOD2, GPX1 and catalase (ab1832, ab18192, ab13533, ab22604 and ab16731; Abcam); total and phospho-Thr68 Chk2, Bax, Bcl-xl (CS3440 2661, 2774, 2764; Cell Signal.). Mitochondrial complex subunits are detected using Total OXPHOS Human WB antibody Cocktail (ab110411, Abcam) containing antibodies against CplxI subunit NDUFB8 (ab110242), Cplx II subunit 30kDa (ab14714), Cplx III subunit Core 2 (ab14745), Cplx IV subunit II (ab110258), and ATP synthase subunit α (ab14748). Densitometric analyses were performed with Biorad software.

2.5. Interleukin-8 quantification

Human Interleukin-8 (IL-8) dosages were performed weekly by ELISA on HMVEC-L supernatants following the company's protocol (Quantikine ELISA kits, R&D).

2.6. Total ROS and superoxide anions quantification

Total ROS and superoxide anions were measured respectively with chloromethyl derivative of 2′, 7′-dichlorodihydrofluorescein diacetate (CM-H2DCFDA) and MitoSOX™ Red (C6827, M36008, Invitrogen) molecular probes. As described by the company's protocol, the fluorescence released by probes oxidation was measured by FacsCalibur (BD) in live cells then analyzed with CellQuest (BD).

2.7. Mitochondrial respiration analysis

HMVEC-L were seeded at 5000 cells/cm^2 in 24-well XF microplate and cultured until reaching confluency. Cells were irradiated in XF microplates and oxygen consumption rate (OCR) was measured 7 days later using XF24 Analyzer (Seahorse), as described in Oizel et al. [22]. Briefly, after cell equilibration in bicarbonate-free DMEM medium supplemented with 25mM glucose, 1mM pyruvate and 2mM glutamine (all Sigma-Aldrich), OCR was measured at baseline and after addition of respectively oligomycin, CCCP, rotenone and antimycin-A (each 0.6μM). Basal OCR was calculated as the mean of the first 4 measures of OCR, before any drug injection, minus OCR after antimycin A corresponding to non-mitochondrial respiration. Cplx I activity was calculated by the subtraction of OCR after rotenone to basal OCR and Cplx II activity by the difference between OCR after rotenone and OCR after antimycin A. All measurements were done in 5 wells per condition per experiment and repeated at least 3 times.

2.8. Mitochondrial morphology and mass quantification

HMVEC-L were incubated with Mitotracker™ Red CMXRos (Invitrogen) for 30 min at 37°C before 4% PFA fixation. Mitochondria morphology was examined on slides counterstained with Prolong Gold DAPI (Sigma) under confocal microscope (Nikon A1 630x magnification). Mitochondrial mass per cell were assessed on 15000 cells by FacsCalibur and CellQuest analysis.

2.9. γH2AX immunostaining

γH2AX immunostaining was performed as described [23]. Briefly, HMVEC-L were seeded at 5000 cells/cm² on glass coverslips coated with 1% gelatin and grown to confluence. One hour, 7 days and 14 days post-15 Gy, cells were fixed in 4% PFA, and permeabilized with 0.1% Triton X-100. Cells were incubated with γH2AX antibody (9718, Cell Signaling) O/N at 4°C, then with anti-IgG-Alexa568 (A11036, Invitrogen) 1 h, at RT and counterstained with Prolong Gold DAPI (Sigma). γH2AX foci number in nucleus section were observed under confocal microscope (Nikon A1 630x magnification) and count was processed using ImageJ (NIH). Number of foci per cell was reported on the total cell number per field representing a mean of 350 cells from 9 fields (3 independent experiments).

2.10. Statistical analysis

Three independent experiments were performed per study. Student's t test and ANOVA with 95% confidence estimation were performed with Prism 6 software.

3. Results

3.1. IR induces senescence in quiescent microvascular endothelial cells, independently of apoptosis modulation by S1P

In this study, microvascular HMVEC-L were used because of their ability to remain in a quiescence phase for several weeks, as observed in normal physiology. We first summarized IR-induced acute apoptosis in this primary endothelial cell model, as previously described in other endothelial cell models [20]. Exposure to 15 Gy induced an early wave of apoptosis within 24h with no further death event in the next 72 h (Fig. 1). Acute apoptosis was inhibited by 40% with a unique pretreatment of 1µM S1P.

Then, long-term senescence was investigated in irradiated HMVEC-L by 4 independent hallmarks: SA β-gal activity, $p21^{Waf1}$ and $p16^{Ink4a}$ expression, IL-8 SASP secretion and persistent DDR activation (Fig.2). The percentage of senescent HMVEC-L expressing SA β-gal (blue staining; Fig. 2A) increased in a dose- and time-dependent manner and reached 63.9%±3.5, day 28 after 15 Gy (vs. 0 Gy; mean %±SEM, $P<0.01$; Fig. 2B). $p16^{Ink4a}$ and $p21^{Waf1}$ expression increased progressively, day 21 after IR (Fig. 2C). Pro-inflammatory IL-8 secretion was significantly increased in HMVEC-L medium in a dose-dependent manner all along the experiment (Fig. 2D). Senescence was finally confirmed by the persistence of DNA damage and the activation of DNA damage response (DDR). Fourteen days after exposure to 15 Gy, cells exhibited a low but significant amount of γH2AX foci (median number of foci per cell: 4 after 15 Gy vs. 0 after 0 Gy; Fig. 2E-F). Because of those residual DNA damages, we then studied the DDR signaling pathway by analyzing expression of both the total and the phosphorylated forms of ATM, DNA-PKcs, and Chk2 (Fig. 2G). All 3 proteins were phosphorylated day 21 after 15 Gy, proving the persistent DDR activation. Altogether, the 4 hallmarks of senescence (SA β-gal

assay, $p16^{Ink4a}$ and $p21^{Waf1}$ expression and IL-8 secretion, γH2AX and DDR activation) demonstrated the long-term senescence outcome of quiescent HMVEC-L at a dose ranging from 1 to 15 Gy. Interestingly, anti-apoptotic S1P did not modulate the expression of these senescent markers in irradiated HMVEC-L (Fig. 2).

3.2. IR induces long-term p53 pathway activation combined with expression of mitochondrial detoxification enzymes and mitochondrial ROS production

Because of its involvement in radiation stress response and the senescence fate, we studied long-term p53 response [24]. Persistent activation of this pathway was confirmed by the concomitant expression of p53 and its related regulator MDM2 and effector $p21^{Waf1}$, in a dose dependent manner by Western blot from day 7 to day 28, regardless to S1P pretreatment (Fig. 3A). DDR involvement in p53 activation was validated by treatment with ATM inhibitor, KU55933, which blocked strongly the expression of p53 and MDM2 and moderately the one of $p21^{Waf1}$, in irradiated HMVEC-L (Fig. 3B). Since p53 is involved in oxidative stress response, we investigated whether ROS could be implicated in IR-induced endothelial cell senescence. In fact, chronic treatment with antioxidant N-acetylcysteine (NAC) after 15 Gy significantly decreased senescence by 37.4%±8.3 (vs. IR+vehicle; mean %±SD, $P<0.01$; Fig. 3C). Then, expression of several important intracellular anti-oxidant proteins was studied by Western blot (Fig. 3D). Interestingly, expression of mitochondrial proteins superoxide dismutase-2 (SOD2) and glutathione peroxidase 1 (GPX1) was increased in a dose-dependent manner from day 7 to day 28, whereas expression of the cytoplasmic catalase did not change. In agreement with our previous results, S1P did not affect anti-oxidant protein expression. Because of its inability to modulate senescence and long-term molecular pathways induced by IR, studies using S1P

pretreatment were excluded to the following experiments. Since mitochondrial antioxidant proteins were up-regulated during IR-induced endothelial cells senescence, total and mitochondrial ROS production were measured day 21 post-15 Gy, using respectively CM-H2DCFDA and MitoSOX™ Red probes. Total ROS were not modulated by IR, whereas mitochondrial superoxide anions (O_2•-) were significantly increased by more than 67.8%±5.2 (vs. 0 Gy; mean %±SD, $P<0.01$; Fig. 3E). Altogether, IR induces long-term p53 activation and mitochondrial oxidative stress in senescent endothelial cells.

3.3. IR-induced persistent mitochondria dysfunctions

Since our results suggest that IR induced mitochondrial dysfunctions, we evaluated the oxygen consumption rate (OCR) after irradiation. Basal OCR was similar in control and in 15 Gy-irradiated HMVEC-L at day 7 (Fig. 4A). Oligomycin and CCCP addition showed that IR did not modify mitochondrial respiration dedicated to ATP production and maximal mitochondrial respiration capacity. To determine the relative contribution of the mitochondrial respiratory chain complexes (Cplx) I and II activities to OCR, oxygen consumption was recorded after sequential addition of rotenone and antimycin A, which inhibit respectively Cplx I and Cplx III. First, addition of rotenone in unirradiated cells showed that nearly 90% of OCR was dependent of complex I, the remaining 10% of OCR relies on Cplx II (Fig. 4B). IR did not significantly affect Cplx I contribution, but decreased Cplx II activity to a barely non-detectable level (15 Gy: 4.4%±1.1 vs. 0 Gy; 13.4%±3.5; mean±SEM; $P<0.01$). Western blot against the labile subunits required for the correct folding of the 5 respiratory chains of the complexes, demonstrated that all complexes were correctly expressed. These results suggest that the decrease of Cplx II

activity in senescent cells was not related to a down-regulation or an abnormal structural conformation (Fig. 4C).

Members of Bcl-2 family are related to mitochondrial homeostasis and senescence [12]. In quiescent HMVEC-L 21 days after IR, Bax and Bcl-xL proteins were up-regulated in a dose-dependent manner whereas expression of Bcl-2 was down-regulated all along the experiment (Fig. 4D). Finally, mitochondrial network disturbance was assessed by observation of the mitochondria morphology using the Mitotracker™ Red CMXRos probe. Quiescent unirradiated cells exhibited a similar mitochondrial network at day 0 and day 21 (Fig. 4E). However, this network was spread out in irradiated cells. This microscopic observation was validated by quantitative FACS analysis showing a 30% increase of the mitochondrial mass 21 days after exposure to 15 Gy (vs. 0 Gy; $P<0.01$; Fig. 4F).

3.4. p53 and mitochondrial O_2•- are implicated in IR-induced endothelial cells senescence in 2 separated pathways

To better characterize their involvement in senescence, pharmacological inhibition of p53 activity and mitochondrial O_2•-, was assessed in HMVEC-L. Chronic treatment with PFT-α, a p53 transcriptional activity inhibitor [25] and/or a manganese metalloporphyrin (MnTBAP), a SOD-mimetic [26], were performed starting 4 days post-IR to avoid potential acute radiosensitization. Here, both inhibitors significantly reduced the SA β-gal positive-staining and the expression of $p21^{Waf1}$ by at least 40% in 15 Gy-irradiated cells (each drug vs. IR-sham; n=3; $P<0.01$; Fig. 5A-B), validating a role for p53 and mitochondrial O_2•- in IR-induced quiescent microvascular endothelial cell senescence. Those results were confirmed with the other senescent marker $p16^{Ink4}$, which was moderately repressed by PFT and strongly by MnTBAP (Fig 5C).

Moreover, co-treatment with both drugs totally reverted senescence. These 2 pharmacological strategies did not modulate the amount of γH2AX foci per HMVEC-L cell 14 days after exposure to 15 Gy as compared to irradiated control (Fig. 5D).

Then, interconnection between p53 and O_2•- was studied. First, p53 overexpression in senescent HMVEC-L was blocked by PFT-α, but not MnTBAP (Fig. 6A). Next, we determined whether mitochondrial O_2•- and mitochondrial Cplx II dysfunction may be connected with p53 pathway. PFT-α treatment did not affect the respiratory Cplx II activity (Fig. 6B) nor the generation of mitochondrial O_2•-, respectively at 7 and 21 days after exposure to 15 Gy (Fig. 6C). Then, we studied the impact of SOD mimetic on mitochondrial dysfunctions. Interestingly, MnTBAP rescued the Cplx II activity (Fig. 6D) and limit the generation of O_2•- (Fig. 6E). Those data clearly demonstrate the discrepancy between 2 senescent pathways involving either O_2•- generation related to mito-dysfunction of respiratory Cplx II or the protein p53.

4. Discussion

Our previous studies highlighted the mechanism of early apoptosis in non-proliferating endothelial cell after exposure to high-dose of IR [8, 20]. In the present study, we now established that confluent non-proliferating endothelial cells also respond to IR by activating a long-term senescence program, through 2 independent mechanisms: the mitochondrial dysfunction associated with oxidative stress and the activation of p53 pathway.

Senescence has already been described in endothelial cells exposed to oxidative stress [13, 27] and ionizing radiation [15-17, 28-30]. However, studies were mainly performed in a model of proliferating macrovascular endothelial cells (HUVEC and BAEC) that poorly reflects the normal physiological vasculature. First, supply of organs with oxygen and nutrients involves the microvascular network that plays a key role in tissue homeostasis. Secondly, endothelial cells in normal tissues are mostly not dividing [18]. We established that death mechanisms induced by IR may differ in endothelial cells depending on their proliferating status [20]. Irradiated quiescent endothelial cells died by apoptosis within hours through ceramide generation, whereas proliferating endothelial cells are also killed within days through a mitotic death triggered by misrepaired DNA breaks. If senescence is clearly observed in proliferating cells after IR, this premature aging in non-dividing endothelial cells remains uncharacterized. Igarishi et al. showed that HUVEC and BAEC irradiated at confluent stage developed senescence [20]. However, senescence was observed when quiescent cells were replated at lower density immediately after IR allowing cells to proliferate. In the present study, we demonstrated that a broad range of therapeutic dose of IR (from 1 to 15 Gy) induces a long-term senescence of non-proliferating microvascular endothelial cells, as shown by several hallmarks: SA β-gal assay, $p16^{Ink4a}$ and $p21^{Waf1}$ protein expression, IL-8 secretion and DDR activation.

Interestingly, our cellular model allows to investigate whereas endothelial cells committed to acute IR-induced apoptosis switch to long-term senescence once their apoptotic program is inhibited. As already described in microvascular SV-40 transformed HMEC-1 [20], we showed in quiescent HMVEC-L that, S1P pretreatment inhibits IR-induced acute cell death (Fig. 1). However, senescence occurred in irradiated endothelial cells, independently of S1P pretreatment, suggesting that IR-induced acute apoptosis and long-term senescence are mediated by 2 distinct pathways. Our results are in agreement with Panganiban and coll., where the blockade of IGF-1R with AG1024 treatment inhibits IR-induced senescence, but not apoptosis [31].

Underlying mechanisms in IR-induced senescence remain under-investigated. The p53/ $p21^{Waf1}$ pathway expression has been predominantly defined as a key actor of H_2O_2- and IR-induced proliferating macrovascular endothelial cell senescence [13, 32]. We also observed the enhancement of the expression of p53 and its related regulator MDM2 and effector $p21^{Waf1}$ during IR-induced quiescent microvascular senescence (Fig. 3A). The fact that PFT-α significantly blocks HMVEC-L senescence, definitely links p53 to IR-induced premature aging. Furthermore, we explain the limited inhibition of $p21^{Waf1}$ and $p16^{Ink4a}$ by PFT-α by a regulation of those senescence biomarkers by a p53-dependent pathway, but also though a mitochondrial-dependent and p53-independent mechanism. In fact, it has been shown that cristacarpin treatment in PANC-1 or MCF-7 promotes endoplasmic reticulum stress, ROS generation and p53-independent senescence defined by SA-β-gal staining and $p21^{Waf1}$ upregulation [33]. Moreover, mutation of TRF2 in primary human fibroblasts induced telomere shortening and replicative senescence involving separately $p16^{Ink4a}$ and p53 [34], 2004). While p53 deficiency alone only partially limited telomere-directed senescence, inhibition of both $p16^{Ink4a}$ and p53 led to nearly complete bypass of the cellular aging. Stabilization of p53 might be triggered through its

phosphorylation on serine 15 residue by the persistence of DDR induced by remaining DNA breaks [35]. During quiescent endothelial cell senescence, ATM, DNA-PKcs and CHK-2, members of the DDR, are still activated after 21 days (Fig. 2G). Moreover, chronic treatment with KU55933, an ATM inhibitor, reduced the expression of p53, MDM2 and $p21^{Waf1}$ (Fig. 3B). These results support a link between the DDR persistent activation and p53 pathway in endothelial cell senescence after IR, in agreement with previous results on H_2O_2-induced vascular aging [13]. Further investigation must definitively decipher the p53-dependent pathway involved in quiescent endothelial cell senescence after IR.

Besides p53 activation, we showed that mitochondrial oxidative stress associated with mitochondrial dysfunctions are involved in IR-induced senescence since both MnTBAP, a SOD mimetic, and NAC, a ROS scavenger, are sufficient to reduce the percentage of SA β-gal-positive senescent HMVEC-L (Fig. 5A & 3C). Our results are in agreement with Kurz and coll., showing that buthionine sulfoxamine, a glutathione synthesis inhibitor, increases intracellular ROS in HUVEC and accelerates replicative senescence [27]. IR induces within milliseconds a rapid and acute H_2O radiolysis leading to a burst of ROS. However, this ROS production is not directly involved in the IR-induced senescence since NAC or MnTBAP treatment start only 4 days post-IR. Endogenous sources of ROS include mitochondria, in particular from respiratory complexes I and III [36]. Yet, succinate-driven oxidation via respiratory Cplx II can contribute significantly to ROS production [37]. In our model, IR alters mitochondrial network, reduces respiratory Cplx II activity and increases mitochondrial O_2•- production. Only a few studies linked Cplx II with aging. None was shown in endothelial cells or after exposure to IR, in contrast to inactivation of complexes I, III and IV that have been noticeably associated with oxidative stress-induced senescence [38]. In particular, Cplx II defect, via down-regulation of its

iron-sulfur succinate deshydrogenase subunit (SDHB) by desferroxamine mesylate induces mitochondrial dysfunction and cell cycle arrest in Chang hepatic cells [38]. However, the inactivation of Cplx II could not be explained in senescent HMVEC-L by a down-regulation of the SDHB subunit expression (Fig. 4C) suggesting that other mechanisms are involved such as its disintegration following intracellular acidification [39], lipid peroxidation [40] or glutathionylation of flavoprotein succinate dehydrogenase subunit (SDHA) induced by O_2•- generation [41]. In fact, we showed that MnTBAP reduces mitochondrial O_2•- generation but also reverts respiratory Cplx II dysfunction. These results demonstrated that, in our model, superoxide anions are involved in Cplx II dysfunction. (Fig. 6C-D). Therefore, we ought to propose a model where a vicious cycle amplifies oxidative stress, with primary O_2•- induces respiratory Cplx II dysfunctions with, in return, increases mitochondrial O_2•- production (Fig. 7). Further investigations must define the primary source of O_2•-. NADPH-oxidase, and xanthine-oxidase complexes might be at the origin of initial burst of O_2•-. Of note, expression of mitochondrial Nox4 was not modified in senescent HMVEC-L after IR (data not shown). The down-regulation of detoxification enzymes may also promote ROS and has been detected during senescence [42]. However, we observed opposite results, where mitochondrial O_2•- generation was correlated with the up-regulation of mitochondrial SOD2 and GPX1 (Fig. 3C). The persistence of mitochondrial oxidative stress and the up-regulation of detoxification enzymes suggest an inability of quiescent endothelial cells to counteract the deleterious effects of IR, leading to the establishment of a chronic stress [43]. Bcl-2 also demonstrates an anti-oxidative property by locating glutathione at mitochondria [12]. Its downregulation in replicative senescent HUVECs enhances the oxidant stress and impairs mitochondrial membrane potential. We also observed Bcl-2 downregulation, which was not modulated by PFT-α- or MnTBAP (data not

shown). We concluded that Bcl-2 may play a role in IR-induced senescence in quiescent HMVEC-L above p53 or in parallel of activation and O_2•- generation.

In our study, we define key roles for the 2 pathways, p53 and O_2•-/Cplx II in IR-induced endothelial cell senescence (Fig. 7). Some studies link the 2 pathways when p53 is activated following ROS-induced DNA damage and ATM phosphorylation [44]. First, in our model, neither MnTBAP nor PFT-α was able to limit the amount of γH2AX foci per cell, proving that p53 and O_2•- pathways were downstream of IR-induced DDR. It has been shown that p53 is also able to inhibit ROS generation by activating the transcription of detoxification enzymes [45]. In our study, PFT-α did not affect the induced expression of SOD2 or GPX1 in irradiated HMVEC-L (data not shown). Moreover, PFT-α surprisingly did not inhibit the long-term dysfunction of respiratory Cplx II or the generation of mitochondrial O_2•- (Fig. 6B-C), demonstrating that mitochondrial redox status was not regulated by long-term p53 over-expression. On the other hand, MnTBAP significantly restores respiratory Cplx II activity, inhibits mitochondrial O_2•- without modulating p53 expression (Fig. 6A, D-E). Altogether, these results show that these 2 pathways are disconnected. This unique result may be due to the singularity of the cell model involving a quiescent primary microvascular endothelial cell and must be explored in other vascular cell models.

Senescence in endothelial cells impairs vascular functions, e.g. pro-inflammatory cytokines secretion, vasotonicity, migration, angiogenesis or permeability [15], known to be involved in chronic pathologies, encountered during aging or long-term radiation toxicity [1]. In this context, we define an active but disconnected roles for p53 and mitochondrial O_2•- / Cplx II generation in senescent primary HMVEC-L after IR (Fig. 7). Their combined pharmacological inhibition should mitigate endothelial cell premature aging, vascular dysfunctions and late radiation

pathologies. However, inhibiting p53 tumor suppressor *in vivo* remains difficult because of potential enhancement of radiation-induced mutagenesis. On the other hand, inhibiting O_2•- by delivering SOD2 with plasmid-liposome or adenovirus has been shown to prevent lung inflammatory alveolitis and fibrosis in irradiated C57BL/6J or Nu/J mice [46]. Further studies should deeply investigate pharmacological drugs against other p53 partners and mitochondrial oxidative stress in order to provide new strategies against endothelial cell aging and to limit chronic radiation toxicity.

Acknowledgment

We thank Denis Cochonneau, Elise Beneteau, the microscopy platform MicroPICell and the cytometry core facility Cytocell for technical help.

Disclosure

The study was founded by the project ProVasc from Région Pays de la Loire, Electricité de France, la Ligue Nationale Contre le Cancer, l'Association de la Recherche sur le Cancer.

Conflict of Interest

No conflict of interest.

Abbreviations

IR: irradiation; ROS: reactive oxygen species; DDR: DNA damage response; SASP: senescence-associated secretory phenotype; O/N: overnight.

Reference

[1] M.H. Gaugler, A unifying system: does the vascular endothelium have a role to play in multi-organ failure following radiation exposure?, BJR Suppl 27 (2005) 100-5.

[2] I. Corre, M. Guillonneau, F. Paris, Membrane signaling induced by high doses of ionizing radiation in the endothelial compartment. Relevance in radiation toxicity, Int J Mol Sci 14(11) (2013) 22678-96.

[3] J. Wang, M. Boerma, Q. Fu, M. Hauer-Jensen, Significance of endothelial dysfunction in the pathogenesis of early and delayed radiation enteropathy, World J Gastroenterol 13(22) (2007) 3047-55.

[4] F. Paris, Z. Fuks, A. Kang, P. Capodieci, G. Juan, D. Ehleiter, A. Haimovitz-Friedman, C. Cordon-Cardo, R. Kolesnick, Endothelial apoptosis as the primary lesion initiating intestinal radiation damage in mice, Science 293(5528) (2001) 293-7.

[5] Y.Q. Li, P. Chen, A. Haimovitz-Friedman, R.M. Reilly, C.S. Wong, Endothelial apoptosis initiates acute blood-brain barrier disruption after ionizing radiation, Cancer Res 63(18) (2003) 5950-6.

[6] L.A. Pena, Z. Fuks, R.N. Kolesnick, Radiation-induced apoptosis of endothelial cells in the murine central nervous system: protection by fibroblast growth factor and sphingomyelinase deficiency, Cancer Res 60(2) (2000) 321-7.

[7] J. Xu, X. Yan, R. Gao, L. Mao, A.P. Cotrim, C. Zheng, C. Zhang, B.J. Baum, S. Wang, Effect of irradiation on microvascular endothelial cells of parotid glands in the miniature pig, Int J Radiat Oncol Biol Phys 78(3) (2010) 897-903.

[8] S. Bonnaud, C. Niaudet, F. Legoux, I. Corre, G. Delpon, X. Saulquin, Z. Fuks, M.H. Gaugler, R. Kolesnick, F. Paris, Sphingosine-1-phosphate activates the AKT pathway to protect small intestines from radiation-induced endothelial apoptosis, Cancer Res 70(23) (2010) 9905-15.

[9] J. Campisi, Cancer, aging and cellular senescence, In Vivo 14(1) (2000) 183-8.

[10] J.P. Coppe, C.K. Patil, F. Rodier, Y. Sun, D.P. Munoz, J. Goldstein, P.S. Nelson, P.Y. Desprez, J. Campisi, Senescence-associated secretory phenotypes reveal cell-nonautonomous functions of oncogenic RAS and the p53 tumor suppressor, PLoS Biol 6(12) (2008) 2853-68.

[11] F. Rodier, J.P. Coppe, C.K. Patil, W.A. Hoeijmakers, D.P. Munoz, S.R. Raza, A. Freund, E. Campeau, A.R. Davalos, J. Campisi, Persistent DNA damage signalling triggers senescence-associated inflammatory cytokine secretion, Nat Cell Biol 11(8) (2009) 973-9.

[12] M. Uraoka, K. Ikeda, R. Kurimoto-Nakano, Y. Nakagawa, M. Koide, Y. Akakabe, Y. Kitamura, T. Ueyama, S. Matoba, H. Yamada, M. Okigaki, H. Matsubara, Loss of bcl-2 during the senescence exacerbates the impaired angiogenic functions in endothelial cells by deteriorating the mitochondrial redox state, Hypertension 58(2) (2011) 254-63.

[13] H. Zhan, T. Suzuki, K. Aizawa, K. Miyagawa, R. Nagai, Ataxia telangiectasia mutated (ATM)-mediated DNA damage response in oxidative stress-induced vascular endothelial cell senescence, J Biol Chem 285(38) (2010) 29662-70.

[14] K. Igarashi, M. Miura, Inhibition of a radiation-induced senescence-like phenotype: a possible mechanism for potentially lethal damage repair in vascular endothelial cells, Radiat Res 170(4) (2008) 534-9.

[15] Z. Ungvari, A. Podlutsky, D. Sosnowska, Z. Tucsek, P. Toth, F. Deak, T. Gautam, A. Csiszar, W.E. Sonntag, Ionizing radiation promotes the acquisition of a senescence-associated secretory phenotype and impairs angiogenic capacity in cerebromicrovascular endothelial cells:

role of increased DNA damage and decreased DNA repair capacity in microvascular radiosensitivity, J Gerontol A Biol Sci Med Sci 68(12) (2013) 1443-57.

[16] Z. Barjaktarovic, N. Anastasov, O. Azimzadeh, A. Sriharshan, H. Sarioglu, M. Ueffing, H. Tammio, A. Hakanen, D. Leszczynski, M.J. Atkinson, S. Tapio, Integrative proteomic and microRNA analysis of primary human coronary artery endothelial cells exposed to low-dose gamma radiation, Radiat Environ Biophys 52(1) (2013) 87-98.

[17] J.I. Heo, W. Kim, K.J. Choi, S. Bae, J.H. Jeong, K.S. Kim, XIAP-associating factor 1, a transcriptional target of BRD7, contributes to endothelial cell senescence, Oncotarget 7(5) (2016) 5118-30.

[18] B. Hobson, J. Denekamp, Endothelial proliferation in tumours and normal tissues: continuous labelling studies, Br J Cancer 49(4) (1984) 405-13.

[19] Y. Morita, G.I. Perez, F. Paris, S.R. Miranda, D. Ehleiter, A. Haimovitz-Friedman, Z. Fuks, Z. Xie, J.C. Reed, E.H. Schuchman, R.N. Kolesnick, J.L. Tilly, Oocyte apoptosis is suppressed by disruption of the acid sphingomyelinase gene or by sphingosine-1-phosphate therapy, Nat Med 6(10) (2000) 1109-14.

[20] S. Bonnaud, C. Niaudet, G. Pottier, M.H. Gaugler, J. Millour, J. Barbet, L. Sabatier, F. Paris, Sphingosine-1-phosphate protects proliferating endothelial cells from ceramide-induced apoptosis but not from DNA damage-induced mitotic death, Cancer Res 67(4) (2007) 1803-11.

[21] G.P. Dimri, X. Lee, G. Basile, M. Acosta, G. Scott, C. Roskelley, E.E. Medrano, M. Linskens, I. Rubelj, O. Pereira-Smith, et al., A biomarker that identifies senescent human cells in culture and in aging skin in vivo, Proc Natl Acad Sci U S A 92(20) (1995) 9363-7.

[22] K. Oizel, C. Gratas, A. Nadaradjane, L. Oliver, F.M. Vallette, C. Pecqueur, D-2-Hydroxyglutarate does not mimic all the IDH mutation effects, in particular the reduced

etoposide-triggered apoptosis mediated by an alteration in mitochondrial NADH, Cell Death Dis 6 (2015) e1704.

[23] V.A. Potiron, R. Abderrahmani, E. Giang, S. Chiavassa, E. Di Tomaso, S.M. Maira, F. Paris, S. Supiot, Radiosensitization of prostate cancer cells by the dual PI3K/mTOR inhibitor BEZ235 under normoxic and hypoxic conditions, Radiother Oncol 106(1) (2013) 138-46.

[24] A. Rufini, P. Tucci, I. Celardo, G. Melino, Senescence and aging: the critical roles of p53, Oncogene 32(43) (2013) 5129-43.

[25] P.G. Komarov, E.A. Komarova, R.V. Kondratov, K. Christov-Tselkov, J.S. Coon, M.V. Chernov, A.V. Gudkov, A chemical inhibitor of p53 that protects mice from the side effects of cancer therapy, Science 285(5434) (1999) 1733-7.

[26] S. Nistico, D. Ventrice, C. Dagostino, F. Lauro, S. Ilari, M. Gliozzi, C. Colica, V. Musolino, C. Carresi, M.C. Strongoli, I. Vecchio, M. Rizzo, V. Mollace, C. Muscoli, Effect of MN (III) tetrakis (4-benzoic acid) porphyrin by photodynamically generated free radicals on SODs keratinocytes, J Biol Regul Homeost Agents 27(3) (2013) 781-90.

[27] D.J. Kurz, S. Decary, Y. Hong, E. Trivier, A. Akhmedov, J.D. Erusalimsky, Chronic oxidative stress compromises telomere integrity and accelerates the onset of senescence in human endothelial cells, J Cell Sci 117(Pt 11) (2004) 2417-26.

[28] C.W. Oh, E.A. Bump, J.S. Kim, D. Janigro, M.R. Mayberg, Induction of a senescence-like phenotype in bovine aortic endothelial cells by ionizing radiation, Radiat Res 156(3) (2001) 232-40.

[29] K.S. Kim, J.E. Kim, K.J. Choi, S. Bae, D.H. Kim, Characterization of DNA damage-induced cellular senescence by ionizing radiation in endothelial cells, Int J Radiat Biol 90(1) (2014) 71-80.

[30] R.A. Panganiban, O. Mungunsukh, R.M. Day, X-irradiation induces ER stress, apoptosis, and senescence in pulmonary artery endothelial cells, Int J Radiat Biol 89(8) (2013) 656-67.

[31] R.A. Panganiban, R.M. Day, Inhibition of IGF-1R prevents ionizing radiation-induced primary endothelial cell senescence, PLoS One 8(10) (2013) e78589.

[32] Z. Barjaktarovic, D. Schmaltz, A. Shyla, O. Azimzadeh, S. Schulz, J. Haagen, W. Dorr, H. Sarioglu, A. Schafer, M.J. Atkinson, H. Zischka, S. Tapio, Radiation-induced signaling results in mitochondrial impairment in mouse heart at 4 weeks after exposure to X-rays, PLoS One 6(12) (2011) e27811.

[33] S. Chakraborty, R.U. Rasool, S. Kumar, D. Nayak, B. Rah, A. Katoch, H. Amin, A. Ali, A. Goswami, Cristacarpin promotes ER stress-mediated ROS generation leading to premature senescence by activation of p21(waf-1), Age (Dordr) 38(3) (2016) 62.

[34] J.J. Jacobs, T. de Lange, Significant role for p16INK4a in p53-independent telomere-directed senescence, Curr Biol 14(24) (2004) 2302-8.

[35] S. Banin, L. Moyal, S. Shieh, Y. Taya, C.W. Anderson, L. Chessa, N.I. Smorodinsky, C. Prives, Y. Reiss, Y. Shiloh, Y. Ziv, Enhanced phosphorylation of p53 by ATM in response to DNA damage, Science 281(5383) (1998) 1674-7.

[36] V.G. Grivennikova, A.D. Vinogradov, Generation of superoxide by the mitochondrial Complex I, Biochim Biophys Acta 1757(5-6) (2006) 553-61.

[37] R. Moreno-Sanchez, L. Hernandez-Esquivel, N.A. Rivero-Segura, A. Marin-Hernandez, J. Neuzil, S.J. Ralph, S. Rodriguez-Enriquez, Reactive oxygen species are generated by the respiratory complex II--evidence for lack of contribution of the reverse electron flow in complex I, Febs J 280(3) (2013) 927-38.

[38] Y.S. Yoon, H.O. Byun, H. Cho, B.K. Kim, G. Yoon, Complex II defect via down-regulation of iron-sulfur subunit induces mitochondrial dysfunction and cell cycle delay in iron chelation-induced senescence-associated growth arrest, J Biol Chem 278(51) (2003) 51577-86.

[39] D. Lagadic-Gossmann, L. Huc, V. Lecureur, Alterations of intracellular pH homeostasis in apoptosis: origins and roles, Cell Death Differ 11(9) (2004) 953-61.

[40] K.B. Choksi, J.E. Nuss, W.H. Boylston, J.P. Rabek, J. Papaconstantinou, Age-related increases in oxidatively damaged proteins of mouse kidney mitochondrial electron transport chain complexes, Free Radic Biol Med 43(10) (2007) 1423-38.

[41] Y.R. Chen, C.L. Chen, D.R. Pfeiffer, J.L. Zweier, Mitochondrial complex II in the post-ischemic heart: oxidative injury and the role of protein S-glutathionylation, J Biol Chem 282(45) (2007) 32640-54.

[42] H. Zhang, Z. Zhai, Y. Wang, J. Zhang, H. Wu, Y. Wang, C. Li, D. Li, L. Lu, X. Wang, J. Chang, Q. Hou, Z. Ju, D. Zhou, A. Meng, Resveratrol ameliorates ionizing irradiation-induced long-term hematopoietic stem cell injury in mice, Free Radic Biol Med 54 (2013) 40-50.

[43] E.I. Azzam, J.P. Jay-Gerin, D. Pain, Ionizing radiation-induced metabolic oxidative stress and prolonged cell injury, Cancer Lett 327(1-2) (2012) 48-60.

[44] A. Borodkina, A. Shatrova, P. Abushik, N. Nikolsky, E. Burova, Interaction between ROS dependent DNA damage, mitochondria and p38 MAPK underlies senescence of human adult stem cells, Aging (Albany NY) 6(6) (2014) 481-95.

[45] P. Drane, A. Bravard, V. Bouvard, E. May, Reciprocal down-regulation of p53 and SOD2 gene expression-implication in p53 mediated apoptosis, Oncogene 20(4) (2001) 430-9.

[46] M. Epperly, J. Bray, S. Kraeger, R. Zwacka, J. Engelhardt, E. Travis, J. Greenberger, Prevention of late effects of irradiation lung damage by manganese superoxide dismutase gene therapy, Gene Ther 5(2) (1998) 196-208.

Figures

Figure 1

IR-induced acute apoptosis in quiescent HMVEC-L is inhibited by S1P pretreatment

Percentage of dead cells after irradiation at 15 Gy, assessed by floating cells assay, 24 and 72 hours after pretreatment with S1P or the vehicle (mean %±SD, *P<0.01, n=3).

Figure 2

IR induces long-term senescence in quiescent HMVEC-L, independently of S1P pretreatment

A) Senescent cells (blue cells) assessed by SA β-gal assay by optical microscopy, day 28 after 15 Gy and S1P pretreatment. Scale Bar: 20 µm. B) Senescent cell percentage from SA β-gal assay counted in function of dose, time and S1P pretreatment (mean %±SD, *P<0.01, n=3). C) $p16^{Ink4a}$ and $p21^{Waf1}$ proteins expression evaluated by Western blot in function of dose and S1P pretreatment, day 21 post-IR (n=3, representative blot). D) Cumulative IL-8 secretion in cellular medium in function of dose, time and S1P pretreatment (mean %±SEM, *P<0.01, n=3). E) γH2AX foci (red staining) observed under fluorescent microscopy, day 14 after 15 Gy and S1P pretreatment. Cells were counterstained with DAPI (blue). Scale Bar: 20 µm. F) Number of γH2AX foci per cell, day 14 post-15 Gy and S1P (mean±SD, n=3). G) Total and phosphorylated forms of DNA damage response members ATM, DNA-PKcs and Chk-2, evaluated by Western blot, day 14 post-15 Gy and S1P (n=3, representative blot).

Figure 3

IR induces long-term p53 pathway activation and mitochondrial oxidative stress response in quiescent HMVEC-L

A) p53, MDM2 and $p21^{WAF1}$ expression, assessed by Western blot in function of dose, time and S1P pretreatment (n=5, representative blot). B) p53, MDM2 and $p21^{WAF1}$ expression assessed by Western blot, day 21 post-15 Gy and KU55933 (n=3, representative blot). C) Percentage of senescent cells chronically treated with NAC after 15 Gy. Senescence was assessed by SA β-gal assay, day 21 post-irradiation (mean %±SD, * P<0.01, n=3). D) Detoxification enzymes SOD2, GPX1 and catalase expression assessed by Western blot in function of dose, time and S1P (n=5, representative blot). E) Quantification of total reactive oxygen species and mitochondrial superoxide, assessed respectively with CM-H2-DCFDA and MitoSOX™ Red by FACS analysis, day 21 post-15 Gy (mean of fluorescence±SD, *P<0.01, n=3).

Figure 4

IR induces persistent mitochondrial dysfunctions in quiescent HMVEC-L

A) Oxygen consumption rate (OCR) in control and irradiated HMVEC-L, day 7 post-15 Gy. Basal OCR as well as OCR following injection of oligomycin, CCCP, rotenone and antimycin A were measured (mean±SD, n=4, *P<0.01). B) Relative contribution of complex I and II to basal OCR in control and 15 Gy-irradiated cells C) Expression of the labile subunits of mitochondrial chain complexes using OXPHOS antibody cocktail, assessed by Western blot, day 7 post-15 Gy (n=3, representative blot). D) Bax, Bcl-xl and Bcl-2 proteins expression, assessed by Western blot, day 7 and 14 post-15 Gy (n=3, representative blot). E) Mitochondrial network assessed by immunostaining with Mitotracker™ Red CMXRos, day 21 post-15 Gy. Cells were counterstained with DAPI (blue). Scale Bar: 20µm. F) Mitochondrial mass per cell quantified by

Mitotracker™ Red CMXRos by Facs assay, day 21 post-15 Gy (mean of fluorescence±SD, *P<0.01, n=3).

Figure 5

Inhibiting p53 activity or superoxide dismutase mimetic blocks IR-induced endothelial cells senescence

A) Percentage of senescent cells chronically treated with PFT-α and/or MnTBAP after 15 Gy. Senescence was assessed by SA β-gal assay, day 21 post-IR. (mean %±SD, *P<0.01, n=6). B) $p21^{Waf1}$ and C) $p16^{Ink4a}$ expression, evaluated by Western blot in PFT-α and/or MnTBAP–treated HMVEC-L, day 21 post-15 Gy (n=6, representative blot). D) Number of γH2AX foci per cell in PFT-α– and/or MnTBAP–treated HMVEC-L, day 14 post-15 Gy (mean±SD, n=3).

Figure 6

SOD mimetic, but not p53 inhibition, rescues mitochondrial dysfunction

A) p53 expression evaluated by Western blot in HMVEC-L treated with PFT-α and/or MnTBAP day 21 post-15 Gy (n=6, representative blot). B-C. Respiratory Cplx II activity and mitochondrial superoxide quantification in PFT-α–treated HMVEC-L, respectively evaluated by Seahorse, day 7 post-15 Gy and by FACS analysis with MitoSOX™ Red, day 21 post-15 Gy (both mean±SD, *P<0.01, n=3). D-E. Respiratory Cplx II activity and mitochondrial superoxide quantification in MnTBAP–treated HMVEC-L, respectively evaluated by Seahorse, day 7 post-15 Gy and by FACS analysis with MitoSOX™ Red, day 21 post-15 Gy (both mean±SD, *P<0.01, n=3).

Figure 7

Graphic model of IR induces long-term senescence in endothelial cells involving 2 separated molecular pathways: mitochondrial respiratory Cplx II dysfunction/superoxide generation and DDR/p53.

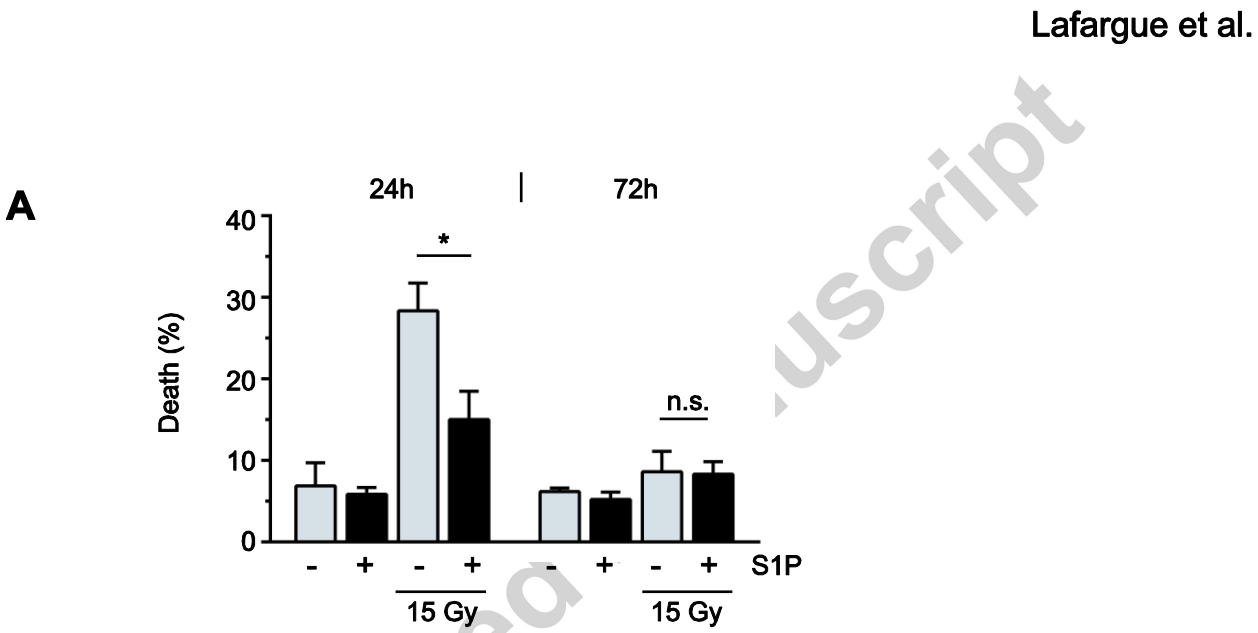

Lafargue et al.

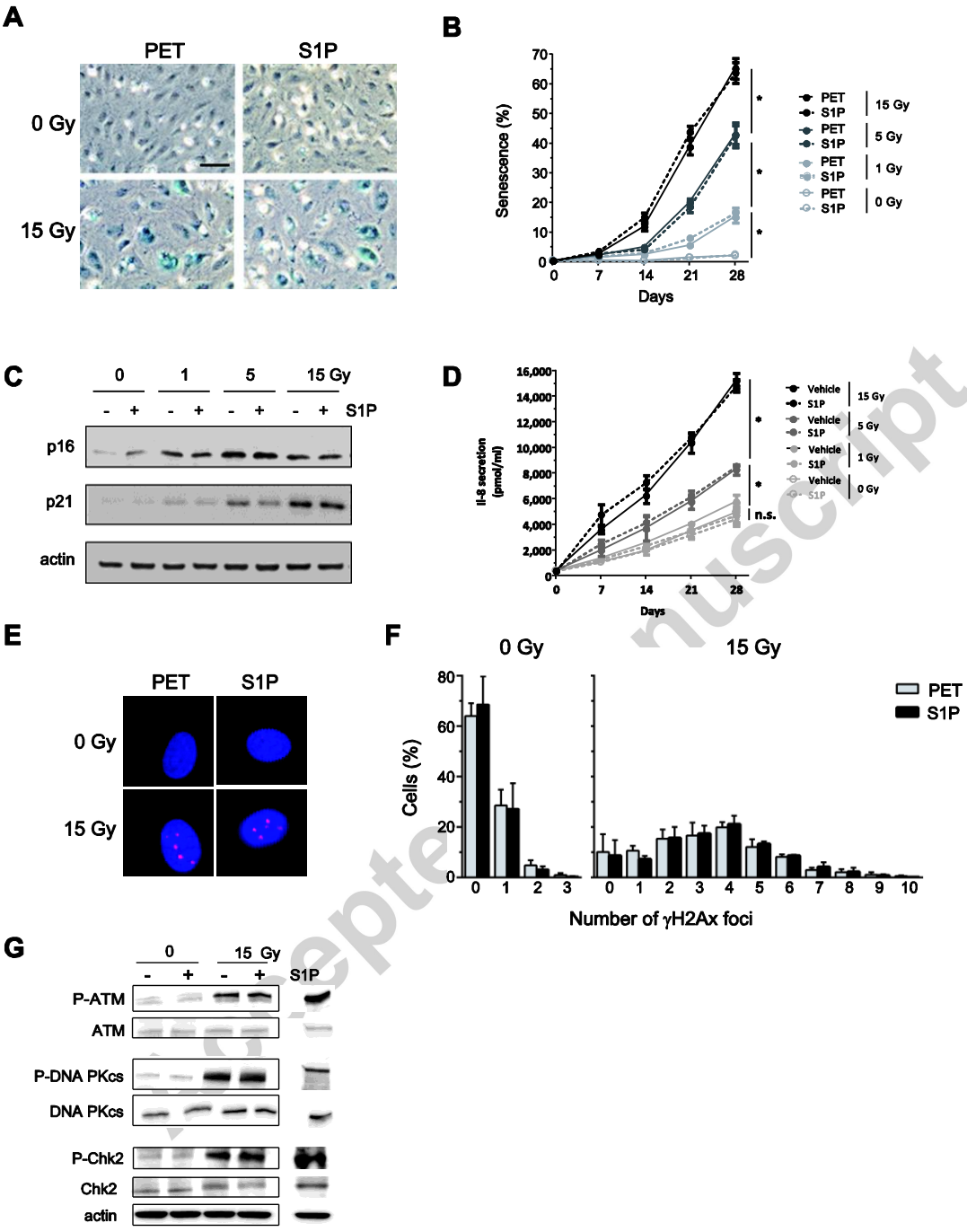

Lafargue et al.

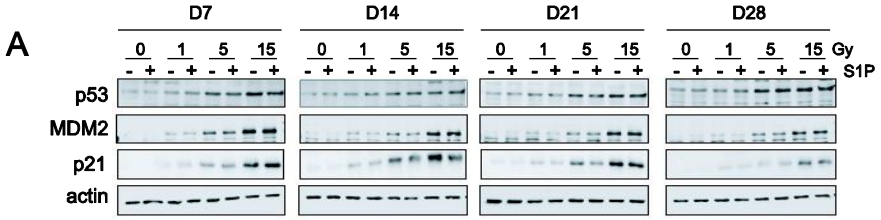

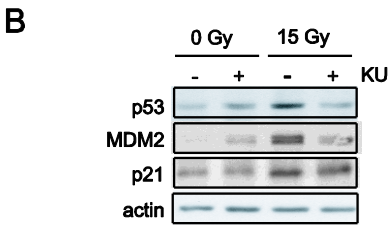

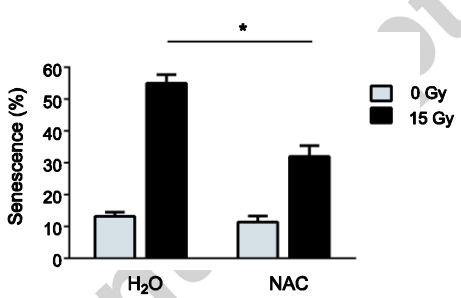

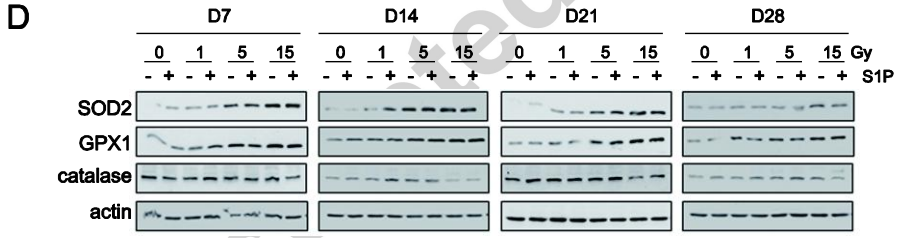

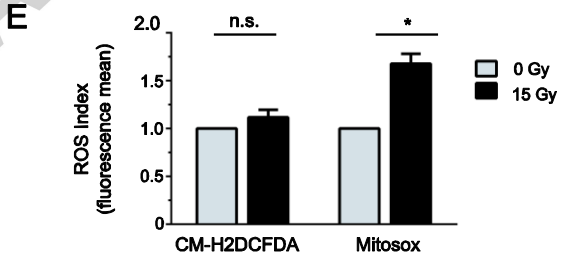

Lafargue et al.

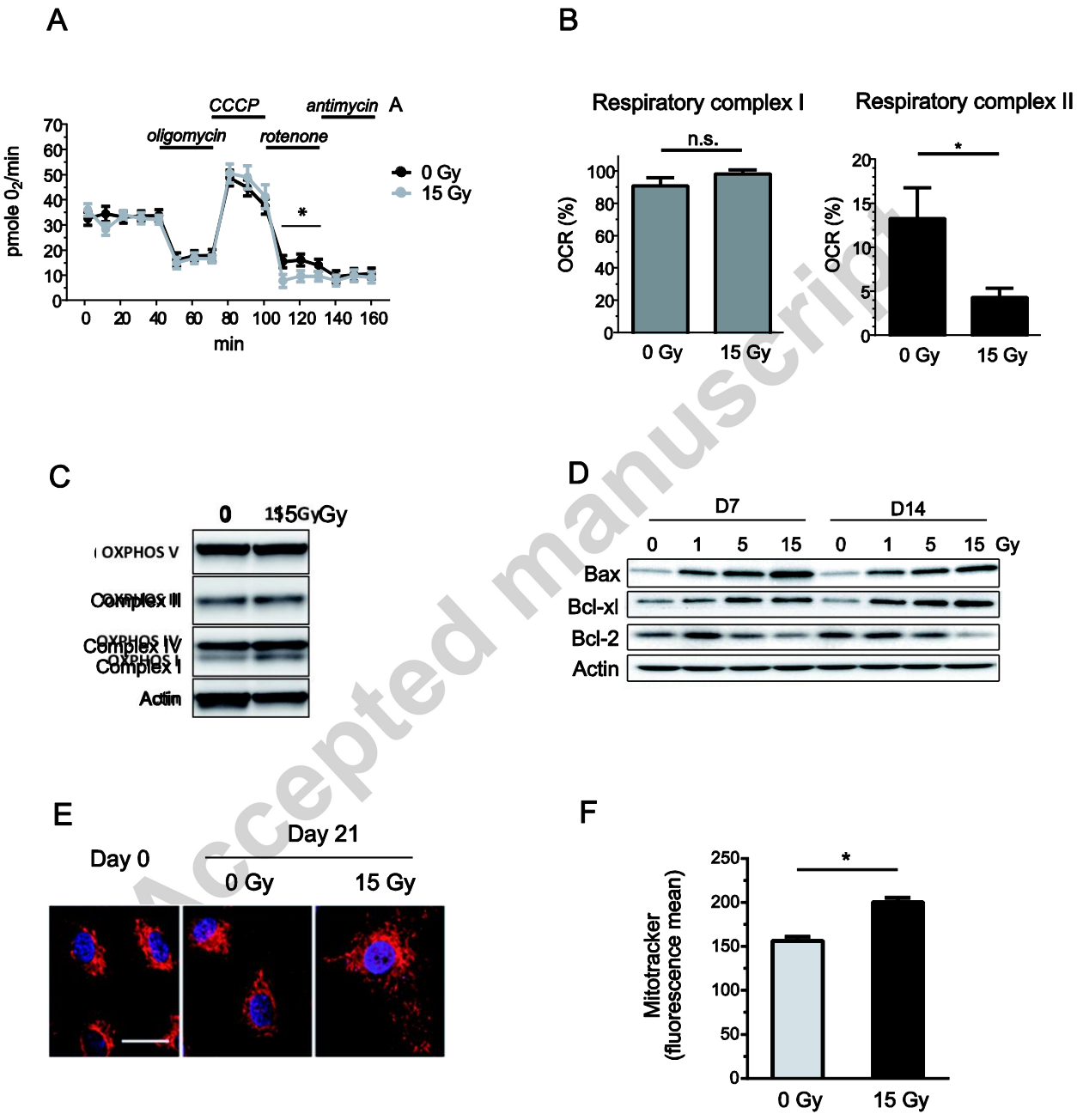

Lafargue et al.

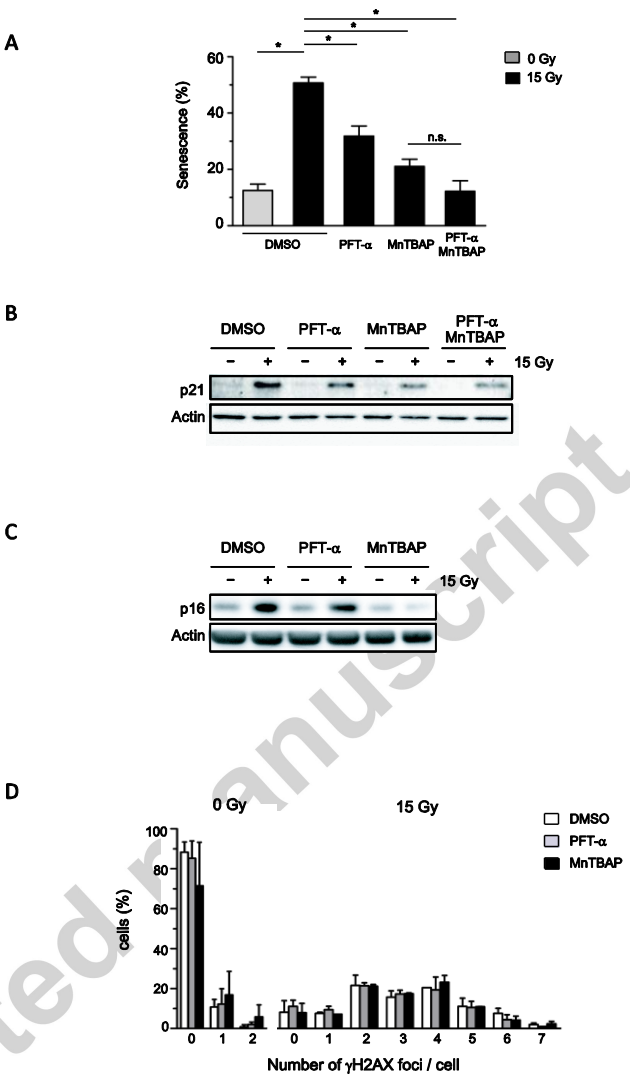

Lafargue et al.